You can view the Version of Record for this article at: https://doi.org/10.1016/j.cej.2020.127179

Low concentration CO_2 capture in fluidized beds of $Ca(OH)_2$ as affected by storage humidity

Helena Moreno [a], Francisco Pontiga [a,*], José M. Valverde [b]

[a] Departamento de Física Aplicada II, ETS Ingeniería de Edificación, Universidad de Sevilla, Av. Reina Mercedes 4, 41012 Sevilla, Spain

[b] Departamento de Electrónica y Electromagnetismo, Facultad de Física, Universidad de Sevilla, Av. Reina Mercedes s/n, 41012 Sevilla, Spain.

* Corresponding author.

E-mail addresses: helena@us.es (H. Moreno), pontiga@us.es (F. Pontiga), jmillan@us.es (J. M. Valverde).

Abstract

Carbon negative emission technologies (NETs) such as CO_2 direct air capture (DAC) are being already considered as necessary for climate change mitigation. This paper investigates CO_2 capture at room temperature and atmospheric pressure by a fluidized bed of $Ca(OH)_2$ powders as influenced by the relative humidity (RH) to which this sorbent was exposed during storage. Humidity is precisely controlled by means of several supersaturared salt solutions, and FTIR spectrometry is used to measure accurately the time evolution of CO_2 and H_2O concentrations in the effluent gas. Results show that CO_2 capture is promoted by an increase of the storage RH. The observed effect is particularly important for very high storage RH (~ 100%, near the dew point). After the capture tests, quantitative analyses of samples composition were carried out using X-ray powder diffractometry. These analyses revealed that the $CaCO_3$ content after CO_2 capture occurs via carbonation in samples that were stored under ~100% RH. On the other hand, in samples stored under low to moderate RH, the presence of $CaCO_3$ was significantly reduced, indicating that most of CO_2 capture takes place through physical adsorption.

Keywords

CO_2 capture; calcium hydroxide; carbonation; direct air capture; pre-hydration; storage conditions; fluidized bed

1. Introduction

The recent UN Climate Change Conference COP 25 held in Madrid in 2019 has urged governments around the world to comply with the recommendation of Paris agreement to keep the global mean temperature rise below 2 ºC relative to pre-industrial levels. Reaching such objective will require strong mitigation measures in all sectors that contribute to CO_2 emissions [1]. In this regard, carbon capture and sequestration (CCS) technologies are being developed to reduce CO_2 emissions from high carbon intensity sources such as fossil fuel based power plants and cement production, where flue gases are released with concentrations of the order of 12-15 vol% [2, 3]. However, because of the limited efficiency of capture technologies, a residual CO_2 concentration is still liberated into the atmosphere ($\leq$ 2 vol%). On the other hand, CCS technologies cannot be used to mitigate distributed CO_2 emissions from other sectors such as transport, residential, agriculture, etc., which account for a significant fraction of total CO_2 emissions (~ 40%) [4].

An increasing number of studies are pointing out that the 2 ºC goal will hardly be achieved without large-scale implementation of carbon negative emission technologies (NETs) during the second half of this century [5, 6, 7]. Sustainable bioenergy with carbon capture and storage has been usually considered the most feasible option of negative-emission technologies [8, 9], albeit direct air capture (DAC) technologies are thought to play a significant role in the mid-term [10,

11]. In fact, some prototypes and commercial DAC plants are already in operation worldwide showing the techno-economic feasibility of this technology with predicted costs below 50 €/tCO_2 by 2040 [12]. Importantly, the increasing levels of CO_2 in the atmosphere is also a concern for the construction sector, since $CaCO_3$ formed in the reaction of CO_2 with $Ca(OH)_2$ in the cement lowers the pH in reinforced concrete structures, which accelerates corrosion [13].

CO_2 capture at low concentration is generally based in the use of a variety of sorbents, such as inorganic chemisorbents (solids or in solution), zeolites, organoamine adsorbents, etc. [14, 15]. Alkaline metal oxides and alkaline earth metal oxides have been reported as good sorbents of CO_2. Calcium-based oxides have the additional advantage of being the most abundant among alkaline earth metal oxides in nature. For that reason, the Calcium Looping (CaL) process, based on the cyclic calcination/carbonation of $CaCO_3$/CaO at high temperature, is gaining attention in the last years to capture CO_2 from high carbon intensity sources, where very large flow rates with a relative high CO_2 vol% (around 15%) must be processed [2, 16, 17]. The need for high carbonation temperatures in this application imposes a fundamental limitation on the capture efficiency, since CO_2 concentration levels in the effluent gas from the carbonator reactor cannot be decreased below the equilibrium CO_2 vol% (around 1% for T ~ 650ºC) [18]. The performance of CaO-based sorbents is also being tested for ambient temperature CO_2 capture from low-CO_2 streams, as potential candidates

for DAC [19]. Although the carbonation reaction is very slow at low temperatures, the CO_2 vol% at equilibrium is virtually zero at ambient temperature, which would allow full CO_2 removal from the inlet gas by using small gas flow rates, considering also the relatively low concentration of CO_2 present in the atmosphere. Thus, recent studies have concluded that, by choosing suitable operating conditions, the use of CaO-based sorbents can be a viable solution for DAC [20].

Among other factors, the relative humidity (RH) in the CO_2 loaded stream is known to play a key role on the capture performance of Ca-based sorbents at low temperatures. Shih et al. [21] investigated the reaction of $Ca(OH)_2$ with CO_2 in humid N_2 at 60-90 ºC. They used a fixed bed reactor, and the bed was humidified before the capture experiments using a certain RH, at which capture was to be performed afterwards. They observed that the reaction of $Ca(OH)_2$ with CO_2 to form $CaCO_3$ only occurs when the RH is above a critical value of 8%. However, since their experiments were carried out with relatively large concentrations of CO_2 (up to 12 %) and high gas flow rates (4 L/min), observations could not be made about the impact of the RH on the CO_2 breakthrough time.

Ridha et al. [19] have conducted a similar research, at room temperature, using lime and pelletized lime-cement particles as sorbents of CO_2. They used a fixed-bed reactor and, before experiments, the sample was hydrated up to 8 hours by

passing through it a flow of humid N_2 at a flow rate of 650 mL/min. Then, CO_2 was incorporated to the humid gas flow in a low concentration that varied from 0.5% to 2%. Although the RH to which the sample was exposed was not measured, their results showed that the pre-hydration phase had a significant effect on the CO_2 capture rate. For example, they observed that the CO_2 breakthrough time was increased from 21 min to 660 min for lime when an inlet concentration of 0.5% of CO_2 was used.

Samari et al. [22] have pursued further this work using an average CO_2 concentration of ~0.04% in the inlet air. They pre-hydrated for 3 h the sample by passing nitrogen through a water bubbler and then through the fixed bed. The air containing CO_2 was then introduced in the reactor using gas flow rates of 0.5 and 1.0 L/min. They observed that the absence of humidity in the inlet air led to a significantly shorter breakthrough time. However, pre-hydration was always perfomed with a single relative humidity (RH ~ 55%).

Dheilly et al. [23] have exposed slaked lime to a controlled atmosphere of CO_2 with different RHs (30%, 60% y 100%), and measured the time evolution of carbonation of $Ca(OH)_2$ for a period of 10 days. The experiments were made inside an environmental chamber, in which the atmosphere was continuously renewed at a rate of 3 L/h. In samples exposed to very low CO_2 concentrations (~0.03%), RH of 30%, and temperature above 20-30 ºC, carbonation of $Ca(OH)_2$ was not observed. However, CO_2 capture occurred progressively as the

ambient RH was raised, and the effect was more intense at the lower temperatures. The authors also conducted other experiments in which $Ca(OH)_2$ was previously humidified in an oxygen atmosphere for 25 days with a RH of 100%. Then, the sample was exposed to the CO_2 loaded atmosphere. They observed a substantial CO_2 capture in the first moments. After 25 days, no more hydroxide was present.

In a very recent paper, Erans et al. [20] have used lime and hydrated lime samples exposed for a prolonged time to ambient air in different environments with the aim of studying its carbonation performance. Small amounts of the samples were periodically analyzed in order to determine their hydration and carbonation degree. They observed that hydrated lime, which was prepared by calcining limestone and then hydrating the sample using a mechanical granulator and deionised sprayed water, captures CO_2 much faster than lime: 50% carbonation conversion was reached in 168 h using hydrated lime, compared to 453 h using lime.

The present work deals with the use of hydrated lime, $Ca(OH)_2$, as CO_2 sorbent from gas streams with low CO_2 concentration at room temperature. In particular, this study aims to investigate the effect of passive pre-hydration on the CO_2 capture performance of $Ca(OH)_2$. As discussed above, the effect of forced pre-hydration of lime and hydrated lime on CO_2 capture has been already considered in previous studies [19, 21, 22]. Forced pre-hydration is usually achieved by

passing a humid gas flow across the sorbent. In contrast, passive pre-hydration consists of a prolonged exposure of the sorbent to a controlled humidity environment, as might occur during sorbent storage in practice. Here, a CO_2-free storage atmosphere will be used during the passive hydration phase, which may lead to hydration but prevents carbonation unlike in other studies [22, 23]. A variety of humidity storage environments will be considered, ranging from a very dry atmosphere (RH 24%) to a very humid one (~ 100%). Additionally, most of previous investigations on CO_2 capture that include pre-hydration also consider the presence of water in the gas stream across the sample during the CO_2 capture test [19, 21, 22]. While this may be advantageous for enhancing CO_2 capture, it can be a confounding factor to determine the role that pre-hydration has played on its own. In this work, CO_2 capture tests will be carried out using a dry mixture of CO_2 (1 vol%) and N_2 at room temperature to prevent the sample from being exposed to additional moisture during CO_2 capture experiments.

The concentrations of CO_2 and H_2O at the exit of the reactor will be continuously and accurately monitored by means of FTIR spectroscopy. This technique allowed us measuring the CO_2 breakthrough time as a function of sorbent storage RH with high precision. Since CO_2 capture can be influenced by the gas-solid contact area, analyses of BET surface area and particle size distribution have been carried out on samples prepared for the capture tests.

After the CO_2 capture tests, the samples have been analyzed by X-ray powder diffractometry in order to measure their $CaCO_3$ content and to know how the capture mechanism is affected by pre-hydration.

2. Materials and sample preparation

The sorbent used in this study was pharmaceutical grade $Ca(OH)_2$ supplied by *PanReac AppliChem*, with a $CaCO_3$ content of less than 5%. As received, this is a cohesive fine powder with micron-size particles that aggregate in clusters of size in the range of tens to hundreds of microns as observed by SEM [24]. Samples of about 4 grams of $Ca(OH)_2$ were prepared and stored in controlled humidity environments following the protocol described below.

Each $Ca(OH)_2$ sample was spread over the bottom of a crystallizing dish (9 cm in diameter) and placed inside a glass desiccator, which would be used as environmental chamber. Inside the chamber, the RH was kept constant using specific supersaturated salt solutions: potassium acetate (CH_3COOK), sodium bromide (NaBr), sodium chloride (NaCl) or potassium sulfate (K_2SO_4). The use of these solutions serves to mimic a diversity of environments in a wide range of RH, from the very dry to the very humid. The container with the salt solution was placed at the bottom of the desiccator, some centimeters below a perforated porcelain disc on whose top rested the crystallizing dish with the $Ca(OH)_2$ sample. A standalone temperature and humidity data logger (*Lascar EL-USB-2-*

LCD) was also left inside the chamber, in order to record at regular intervals both magnitudes. The desiccator was then hermetically sealed, and the air was pumped out and replaced with nitrogen (purity > 99.999%) at 1 bar of absolute pressure, so that carbonation did not occur during passive hydration. Each $Ca(OH)_2$ sample was kept inside the desiccator at room temperature (~ 22 ºC) for six days, which is long enough to ensure that equilibrium with ambient humidity had been reached. The registered values of RH using the above-mentioned supersaturated salt solutions were 24 ± 2%, 58 ± 2%, 75.5 ± 2% and 100 ± 3%, respectively, which agree, within the expected uncertainty, with the values reported in [25]. Shorter storage periods of the sample inside the desiccator resulted in poorer reproducibility of the experiments.

At the end of the passive hydration phase, the $Ca(OH)_2$ sample was extracted from the desiccators and immediately prepared for their use in the CO_2 capture test, in which a gas stream with a low concentration of CO_2 is passed across the sorbent bed. Among other factors [21, 26, 27, 28], the carbonation reaction kinetics is strongly affected by the gas-solid contact surface available for the reaction. Since the fluidization behavior of the $Ca(OH)_2$ powder used in our study belongs to the Geldart C category [29], stable gas channels can easily develop during the passage of gas through the bed. As a consequence, a large part of the gas flow may bypass the bed through these channels, thus hindering the gas-solid contact effectiveness. To avoid this inconvenience, hydrophobic

fumed nanosilica (*Aerosil R974*, from Evonik Industries), with tamped density of about 50 kg/m^3 and specific surface area of the order of 200 m^2/g, was used as additive to improve the fluidization quality of the $Ca(OH)_2$ samples. This nanostructured powder is produced by flame synthesis at high temperatures, which leads to the formation of indestructible porous aggregates of nanoparticles by fusing of the contacts [30], typically of size in the order of one micron. These aggregates tend to form agglomerates of larger size (tens of microns) as the result of weak interactions, such as the attractive van der Waals force.

When hydrated $Ca(OH)_2$ is mixed with *Aerosil R974*, gas channels are destabilized and fluidization is greatly enhanced, which dramatically improves the gas–solid contact efficiency [31]. Previous studies have shown that a mass percentage of 15% wt of nanosilica gives satisfactory results [24, 31, 32]. Therefore, the $Ca(OH)_2$ samples to be tested for CO_2 capture were always prepared by hand dry-mixing the hydrated lime with the nanosilica powder in that percentage.

3. Characterization

As previously stated, CO_2 capture is very sensitive to the gas–solid contact surface available for the carbonation reaction. In order elucidate whether hydration of $Ca(OH)_2$ during storage might have an impact of the surface

properties of samples prepared for the capture tests, measurements of the surface area and particle size were carried out on three selected samples. Two of these samples were prepared using $Ca(OH)_2$ stored at the two most extreme humidity conditions (RH 24 % and RH 100 %). For the third sample, $Ca(OH)_2$ was directly taken from the container, in which RH was about 50 %.

Nitrogen isotherm adsorption/desorption at 77 K was used for measuring the surface area (*Micromeritics ASAP 2420*). Adsorption/desorption plots are shown in figure 1 where, as usual, the volume of adsorbed N_2 (reduced to STP) per unit of adsorbent mass is represented as a function of the ratio of the equilibrium pressure to the saturated vapor pressure of N_2. According to the IUPAC classification [33], these isotherms can be categorized as Type II in the adsorption branch, with a Type H3 hysteresis on desorption. This type of hysteresis is attributed to capillary condensation between non-porous plate-like particles, and has also been reported by other authors for $Ca(OH)_2$ [34]. The multipoint Brunauer-Emmett-Teller (BET) method can be applied to the adsorption isotherms to determine the surface area of the samples. Results from this analysis are presented in table 1: the higher the RH during storage the larger the surface area. Moreover, the fact that the area of the hysteresis loop gets larger for samples stored at higher RH also indicates a progressive increase in mesoporosity.

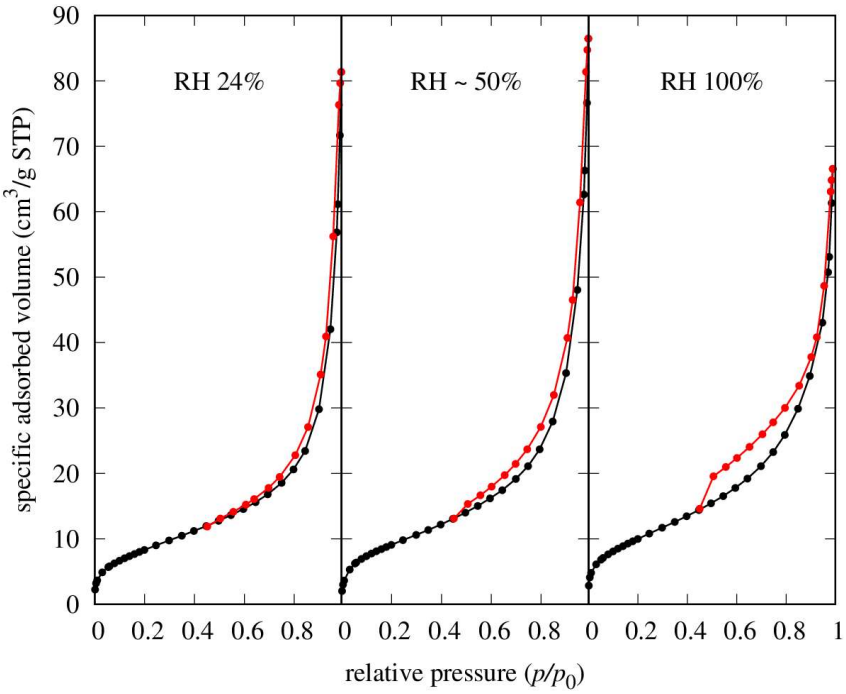

Figure 1: Physisorption isotherms of N_2 at 77 K for selected samples prepared for the CO_2 capture tests using $Ca(OH)_2$ stored at different values of the relative humidity. Black dots: adsorption isotherm. Red dots: desorption isotherm.

RH (%)	BET surface area (m^2/g)	*D* [3,2] (μm)	*D* [4,3] (μm)
24	30.9 ± 0.3	1.9	9.5
~ 50	33.4 ± 0.3	1.9	9.8
100	36.9 ± 0.3	2.2	11.5

Table 1: BET surface area and mean particle diameters (volume and surface weighted) of selected samples prepared for CO_2 capture tests using $Ca(OH)_2$ stored at different relative humidities.

Particle size distributions (PSD) of powder samples prepared for the capture test were obtained by laser diffraction technique, using dry dispersion in a gas jet (*Malvern, Mastersizer 2000*). Figure 2 shows the volume PSD measured for the three samples analyzed. The PSD of the sample stored at RH 100% is slightly shifted towards larger sizes, which may be due to the persistence of some large aggregates held together by intense capillary forces between the particles that could not be overcome by dry dispersion. In any case, SEM images do not reveal a significant difference between samples stored at different RHs (figure 3). The volume-weighted mean diameter (De Brouckere mean diameter) $D[4,3]$, and the surface-weighted mean diameter (Sauter mean diameter) $D[3,2]$, are given in table 1. As can be seen, the storage RH does not essentially affect the particle size.

Finally, measurements of the true (or absolute) density of samples were carried out using helium picnometry (*Quantachrome, Pentapycnometer 5200E*). No substantial differences between samples were found. The averaged true density of the samples was (2.465 ± 0.009) g/cm^3.

Arguably, the presence of adsorbed moisture on the $Ca(OH)_2$ particles can alter the adhesive forces between particles [35], which may affect the fluidization behavior of samples and, therefore, the gas–solid interaction. As explained above, $Ca(OH)_2$ was mixed with hydrophobic fumed nanosilica to improve its fluidizability by decreasing powder cohesiveness. Nanosilica addition leads to a

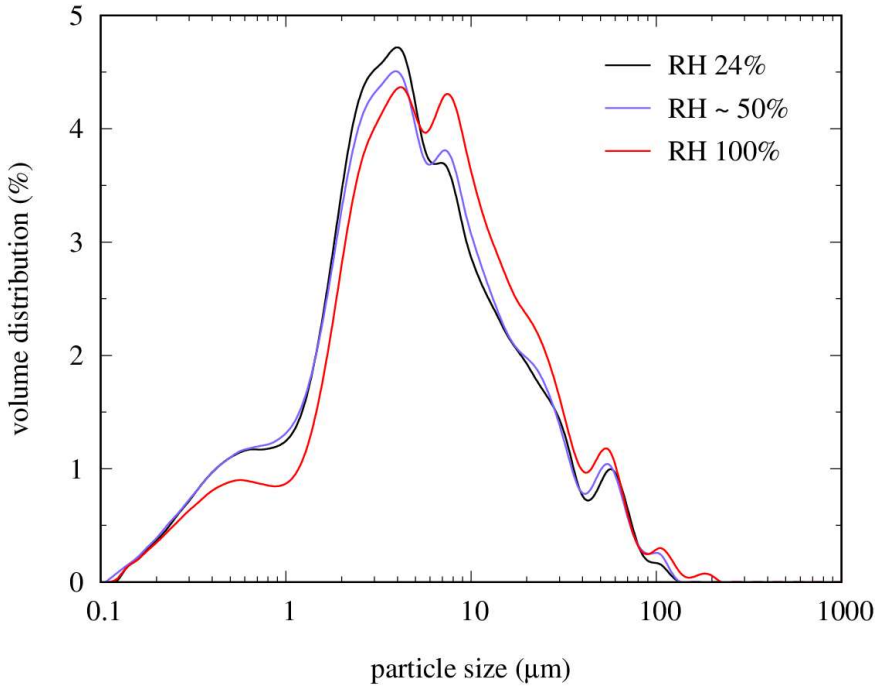

Figure 2: Frequency curve of the volume of particles as a function of the particle size in selected samples prepared for CO_2 capture tests using $Ca(OH)_2$ stored at different relative humidities as indicated.

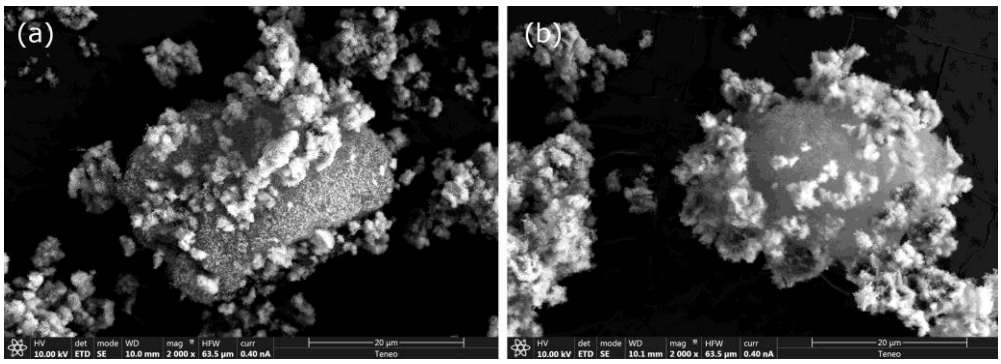

Figure 3: SEM images of nanosilica agglomerates (grey) covered by $Ca(OH)_2$ particles (white) of two selected samples prepared for the CO_2 capture test. (a) $Ca(OH)_2$ stored at RH 24%. (b) $Ca(OH)_2$ stored at RH 100%.

significant reduction in the strength of attractive van der Waals forces between the particles, as shown in previous works [36]. Moreover, the hydrophobicity of nanosilica is expected to minimize the role of adsorbed moisture on the fluidization of the samples used in this study compared to raw $Ca(OH)_2$. In order to test the possible effect of moisture on the powder fluidization behavior, three samples were prepared using $Ca(OH)_2$ stored at different RH (24%, 75.5% and 100%), and their bed expansion curves were measured. These measurements were carried out using dry N_2, and following the same procedure as in CO_2 capture tests. That is, an initial gas flow rate of 1 slpm was imposed through the sample for a period of 3 minutes to initialize the sample in a reproducible state. Then, once the gas flow had stopped and the sample had settled, the gas flow rate was increased in steps 0.01 slpm every 15 s. The results of these tests are shown in figure 4. As can be seen, the relative bed expansions of the samples stored at RH below 100% follow a close trend. At flow rates above 0.2 slpm, the bed expansions reach a plateau, which is higher for the sample stored at 100% RH. Presumably, a high level of humidity can enhance fluidization because it hinders surface tribocharging, which might lead to attractive forces between the particles and between the powder and the internal vessel walls, as seen from visual inspection in figure 5. In CO_2 capture experiments, a flow rate of 0.1 slpm was used in all tests, for which a bubble-free fluidization is observed. At this flow rate, the samples prepared using the $Ca(OH)_2$ stored at RH 24% and 75.5%

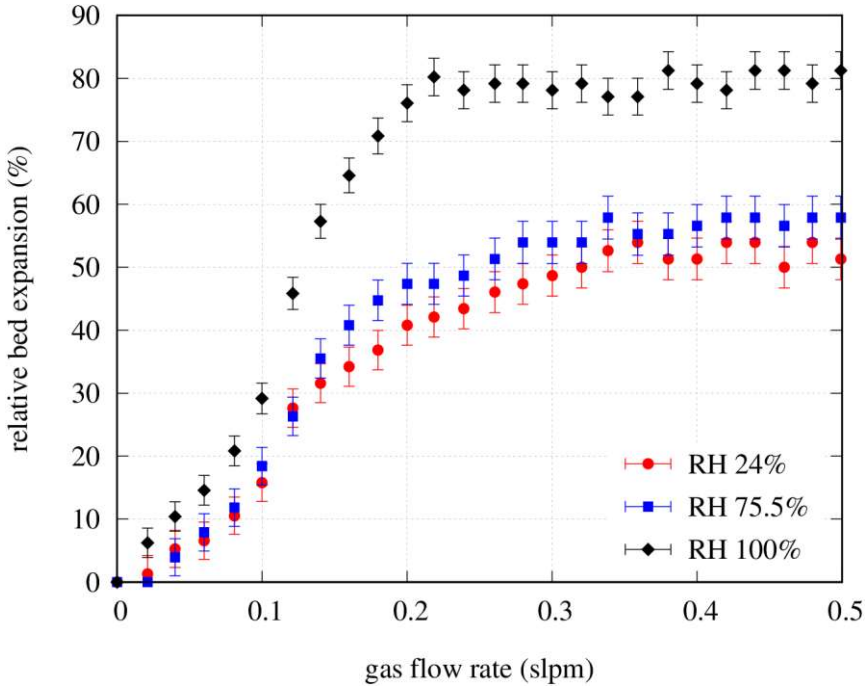

Figure 4: Relative bed expansion as a function of the gas flow rate of $Ca(OH)_2$/nanosilica powder mixtures employed in the CO_2 capture tests, which were prepared using $Ca(OH)_2$ stored at different relative humidities as indicated.

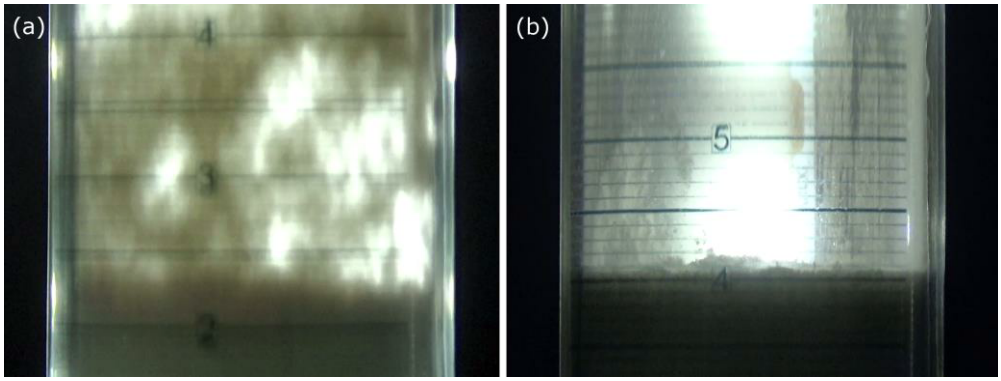

Figure 5: Photographs of the fluidized bed in $Ca(OH)_2$/nanosilica samples prepared with $Ca(OH)_2$ stored at (a) RH 24% and (b) RH 100%, for a gas flow rate of 0.1 slpm.

exhibit very similar values of the relative bed expansion: (16 ± 3)% and (18 ± 3)%, respectively. In contrast, the sample prepared using $Ca(OH)_2$ stored at RH 100% shows a higher relative bed expansion, (29 ± 2)%, which would favor the gas-solid interaction and therefore promote further CO_2 capture.

4. Experimental set-up

Figure 6 shows a schematic representation of experimental set-up used in the experiments. The powder bed was confined in a 20 cm long glass tube, with inner diameter of 23.4 mm. The bottom side of the glass tube was closed with a glass microfiber filter (Whatman Grade GF/A), with a nominal particle retention of 1.6 μm. The sample to be tested (3.45 grams) was deposited upon the glass microfiber filter, which was replaced after every test. The exit of the glass tube was closed with a foam filter, to prevent elutriated particles from exiting the fluidized bed reactor. An additional external pneumatic filter (filtration size 0.01 μm) was inserted between the reactor and the Fourier-transform infrared (FTIR) spectrophotometer (*Bruker Vertex 70*) that was used for the gas analysis. In order to help fluidization of the sample, the reactor was placed on a vibration exciter (*TIRA TV51110*), which was driven with a frequency of 50 Hz. Dry N_2 (gas purity > 99.999%) and CO_2 (gas purity > 99.995%) were employed for the CO_2/N_2 mixture. A system of three mass flow controllers (*Alicat MC-5SLPM-D, MC-200SCCM-D, MC-2SCCM-D*) and solenoid valves were used to prepare the mixture of these gases and to divert the flow either directly to the

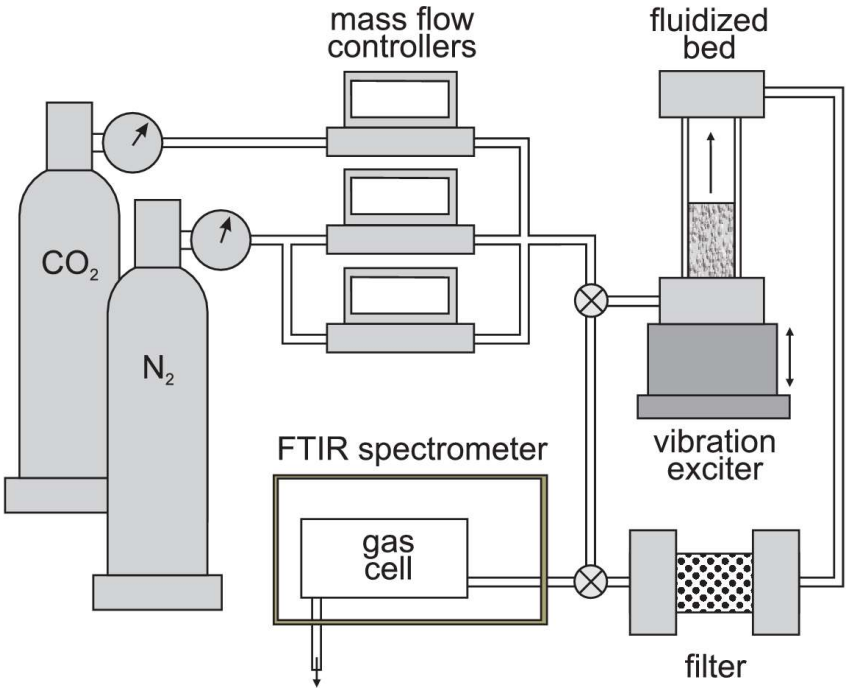

Figure 6: Experimental setup used in the CO_2 capture tests by a fluidized bed. CO_2 and H_2O are detected in the effluent gas by means of a FTIR spectrometer.

spectrophotometer or to the bed reactor and then to the spectrophotometer.

The CO_2 capture experiment was carried out at room temperature and atmospheric pressure as follows. Firstly, a gas flow of 1 slpm of N_2 was imposed through the sample for a period of 3 minutes, in order to initialize the sample in a reproducible state. Then, a gas mixture of 1% CO_2 and 99% N_2, with a gas flow rate of 0.1 slpm, was sent directly to the spectrophotometer, and the absorption spectrum was registered to obtain a calibration reference for this combination of gases. Finally, the same gas mixture and flow rate was diverted

towards the bed reactor, and the effluent gas was analyzed in the spectrophotometer. During this period, IR spectra were recorded every 40 s, in order to track the temporal evolution of the CO_2 and H_2O contents in the gas leaving the reactor. The timestamp of each FTIR spectrum was later corrected for the finite transit time of the gas from the reactor to the spectrometer cell. This transit time was measured at the end of the CO_2 capture experiment. To this purpose, the CO_2/N_2 gas flow was suddenly replaced by pure N_2, and the elapsed time span to observe this change on the FTIR spectra was measured. A transit time of 85 s was obtained.

The infrared spectrophotometer used in the experiments has a spectral resolution better than 0.16 cm^{-1}, which allows the individual peaks in CO_2 and H_2O spectra to be accurately resolved. The uncertainty in CO_2 vol% measurements was below 10 ppm. The optics and the sample compartments of the FTIR spectrophotometer were continuously purged with CO_2-free (less than 1 ppm) ultra-dry air (−73 ºC dew point) to minimize the interference of ambient CO_2 and water vapor. Prior to the tests, the base line of the spectrophotometer was recorded after filling the gas cell with N_2 in order to suppress the contribution of any impurity that might be present in the buffer gas. For the spectral determination of H_2O vol% in the effluent gas, a calibration curve was previously built using a dew point and pressure transmitter (*Vaisala DPT146*).

Finally, X-ray powder diffractometry (*Bruker D8 Advance A25*) was used as a

complementary technique to analyze the composition of some samples after the CO_2 capture tests. Rietveld refinement technique was applied to quantify the percentage of calcite ($CaCO_3$) and portlandite ($Ca(OH)_2$) in these samples.

5. Experimental results and discussion

In order to assess the effect of passive pre-hydration on the CO_2 capture capacity of hydrated lime for its use in DAC, a gas mixture with low CO_2 concentration (1% in volume) was used in all the experiments. Figure 7 shows the time evolution of the CO_2 volume fraction at the exit of the reactor for $Ca(OH)_2$ samples, previously stored in inert environments of different RH levels following the procedure described in section 2. As can be seen, CO_2 is completely removed from the inlet gas stream for a certain period of time (the so-called breakthrough time, BT), which depends critically on the RH storage conditions. Once complete CO_2 capture is ended, the CO_2 vol% in the effluent gas raises very fast in a short period of just a few seconds, after which it approaches asymptotically the CO_2 vol% in the inlet gas mixture. As shown in previous works [24, 31, 32], the sharp rise of CO_2 after the BT is helped by the nanosilica additive added to the sorbent, which promotes the gas-solid contacting efficiency. The phase of complete CO_2 capture until BT is then prolonged in time, and CO_2 appears abruptly in the effluent gas once the reaction sites become saturated. Arguably, this special feature would facilitate in practice switching on/off the capture/sorbent regeneration regimes. As it will be

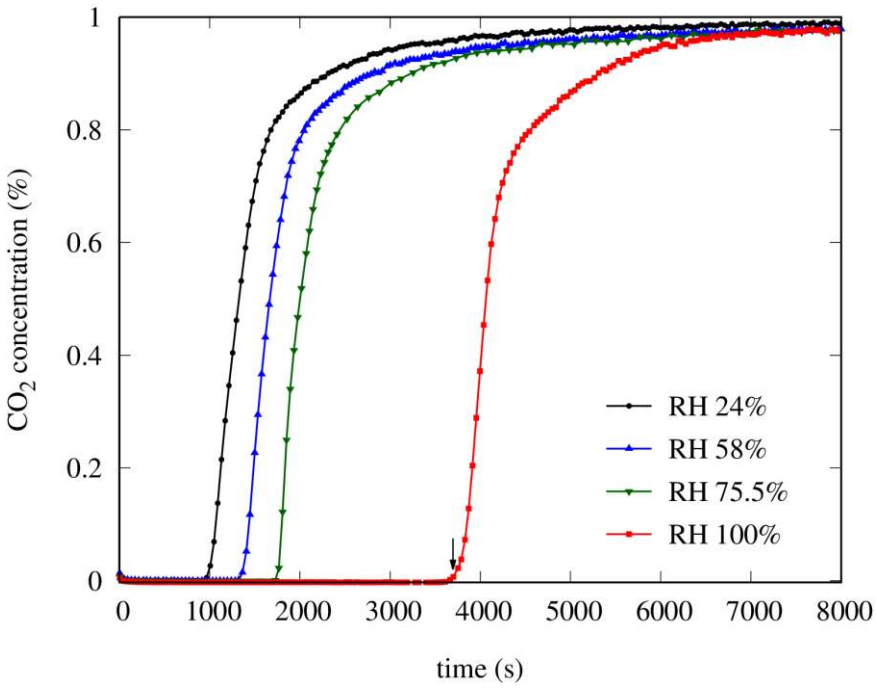

Figure 7: Time evolution of CO_2 volume fraction in the effluent gas during CO_2 capture by a bed of $Ca(OH)_2$ fluidized with a dry CO_2/N_2 gas mixture (1 vol.% CO_2). Calcium hydroxide samples were stored at different RH levels, as indicated. The vertical arrow points to the breakthrough time corresponding to the sample stored at RH of 100%.

shown later, most of CO_2 capture takes place before the BT, when the effluent gas is completely CO_2 clean.

The influence of the RH during the storage of $Ca(OH)_2$ on the breakthrough time can be clearly appreciated in figure 8. For values of the storage RH up to 75.5%, the BT and, therefore, the capture capacity of samples, increases moderately as the storage RH is raised. In contrast, the sample stored at a RH close to the dew point (RH ~ 100%) exhibits a BT substantially higher than the

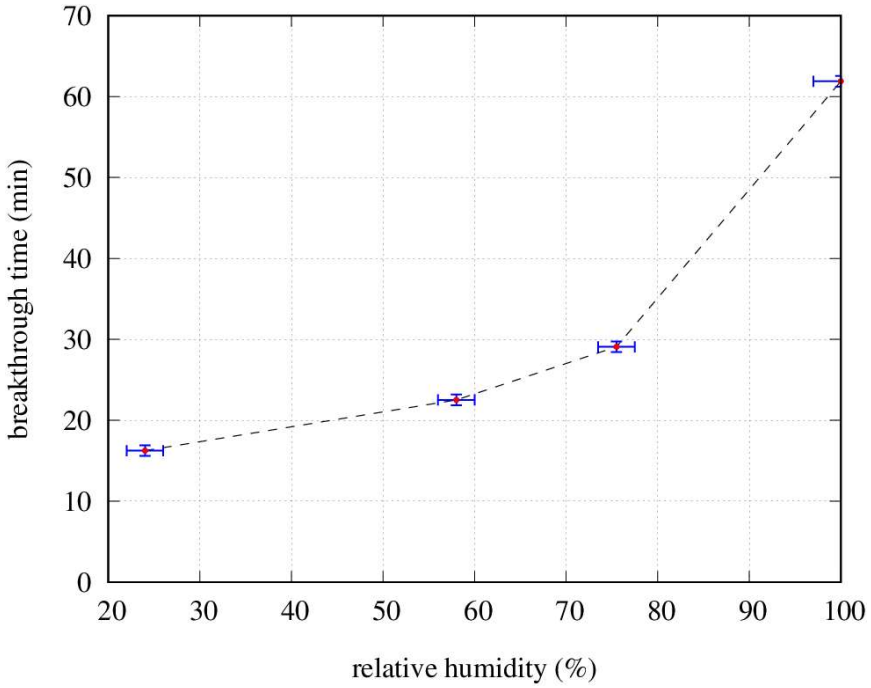

Figure 8: Breakthrough time (BT) measured in the CO_2 capture tests as a function of the relative humidity at which the sorbent was previously stored.

rest of samples: more than twice of that found at a storage RH of 75.5% and more than three times the BT observed at storage RH of 24%.

The surface of sorbent actually exposed to CO_2 is a main limiting factor for the capture reaction. As shown in section 3, both the BET surface area and the mean diameter of sample particles tend to increase slightly with the RH to which $Ca(OH)_2$ was exposed during the pre-hydration phase. However, the increase of surface area of samples with RH was very small and approximately linear, which does not explain the highly nonlinear augmentation of the BT measured during CO_2 capture tests for samples stored at very high RH. In contrast, bed

expansion in samples exposed to very high RH (~ 100%) was found to be higher than in the rest of samples (figure 4). Expectedly, the enhancement of fluidization facilitates further CO_2 capture by promoting the gas-solid interaction.

However, the present results seem to be more consistent with the findings by Beruto and Botter [26]. These authors measured the equilibrium adsorption isotherm of H_2O on $Ca(OH)_2$ at 20 ºC, and observed a smooth linearly increase of water adsorption in the range of relative pressures from 20% to 70%. Then, for RH above 80%, the rate of water adsorption increased very sharply. That result is indicative of the formation of a thick multilayer adsorbed film of H_2O, which behaves as a bidimensional liquid-like interface that facilitates the reaction of CO_2 with $Ca(OH)_2$. It has been argued that the physicochemical processes leading to the carbonation of $Ca(OH)_2$ at low temperatures consist of several steps mediated by the presence of physisorbed water [26, 37]. Firstly, $Ca(OH)_2$ is partially dissolved and dissociated inside adsorbed water layers, releasing Ca^{2+} and OH^- ions,

$$Ca(OH)_{2(s)} \rightleftarrows Ca^{2+}_{(aq)} + 2OH^-_{(aq)} \quad (1)$$

and rendering the solution alkaline. Since CO_2 is slightly soluble in H_2O at low temperatures, aqueous $CO_{2(aq)}$ is formed, and its reaction with the liquid H_2O layer gives rise to carbonic acid,

$$CO_{2(aq)} + H_2O_{(aq)} \rightleftarrows H_2CO_{3(aq)} \quad (2)$$

Dissociation of $H_2CO_{3(aq)}$ produces bicarbonate and carbonate ions and lowers the H_2O alkalinity

$$H_2CO_{3(aq)} \rightleftarrows H^+_{(aq)} + HCO_3^-{}_{(aq)} \quad (3)$$

$$HCO_3^-{}_{(aq)} \rightleftarrows H^+_{(aq)} + CO_3^{2-}{}_{(aq)} \quad (4)$$

However, if water alkalinity is sufficiently elevated, $CO_{2(aq)}$ can also react with hydroxyl ions to directly form bicarbonate ions,

$$CO_{2(aq)} + OH^-_{(aq)} \rightleftarrows HCO_3^-{}_{(aq)} \quad (4)$$

Finally, reaction between Ca^{2+} and CO_3^{2-} leads to the formation and precipitation of calcium carbonate,

$$Ca^{2+}_{(aq)} + CO_3^{2-}{}_{(aq)} \rightleftarrows CaCO_{3(s)} \quad (5)$$

The concentration of dissolved carbonate species depend on the pH of the adsorbed water [38]. At a pH > 10.3, the predominant ion is CO_3^{2-}, which favors carbonation. On the contrary, if water alkalinity is lower, HCO_3^- is more abundant and the formation of $CaCO_3$ proceeds slowly.

The overall reaction can then be written as

$$Ca(OH)_{2(s)} + CO_{2(g)} \rightleftarrows CaCO_{3(s)} + H_2O_{(aq)} \quad (6)$$

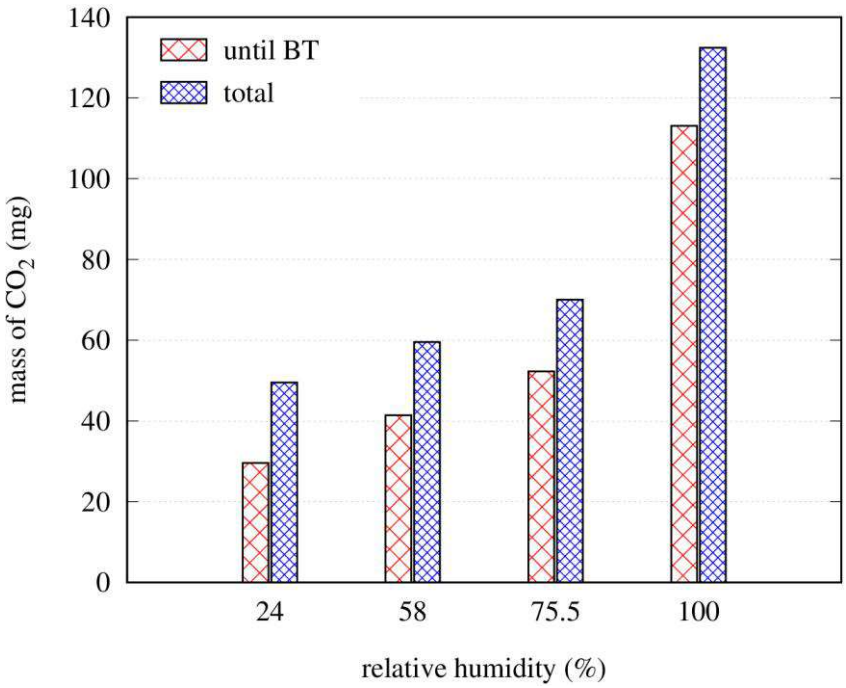

Figure 9: Mass of CO_2 captured by $Ca(OH)_2$ samples previously stored at different RH conditions, as indicated. Red: CO_2 uptake up to breakthrough time. Blue: total CO_2 uptake.

Therefore, the increase of the BT (and CO_2 capture capacity) with the RH used during the hydration phase agrees with this mechanism, in which the amount of physisorbed water and, particularly, the formation of adsorbed film of liquid-like water, is the most determinant factor.

The mass of CO_2 captured during our tests has been obtained by integrating in time the CO_2 vol% measured in the effluent gas. The results are presented in figure 9, where the CO_2 uptake before BT is shown as red bars and the total CO_2 uptake as blue bars. As it can be readily seen, the mass of CO_2 captured after the BT is roughly independent of the storage RH. Therefore, the CO_2 uptake for $t <$

sorbent	pre-hydration	RH (%)	inlet CO_2 (vol%)	pressure (bar)	flow rate (cm^3/min)	BT (min)	Ca (g)	CO_2/Ca (%)
CaO [22]	forced (3h)	~ 55	0.0415	2	1000	~ 24	2.04	1.7
$Ca(OH)_2$	passive	58	1	~ 1	100	~ 23	1.62	2.6

Table 2: Comparison between CO_2 capture tests reported by Samari et al [22] and in this work. The last column shows the mass of CO_2 captured in the experiment per unit of mass of Ca of the sorbent.

BT becomes progressively more important as the storage RH is raised. When the storage RH of about 100%, the CO_2 uptake for t < BT accounts for about 85% of the total CO_2 capture.

It is not straightforward to compare the present results with those from previous studies in which a pre-hydration phase was included before the CO_2 capture test. As it has been already discussed, the experimental conditions are usually very different and, with the aim of maximizing CO_2 capture, humidity is often added to the CO_2 gas stream passing across the sample during the capture test. However, the work of Samari et al. [22] contains enough detail to allow a comparison with our findings (see table 2). These authors used natural lime as sorbent, with a CaO content of 89.57 wt%. Before the capture test, the sorbent was hydrated by passing across the sample a flow of N_2 + H_2O, with RH of about 55%, for 3 hours. Then, the capture test was carried out using compressed

air, with an average CO_2 concentration of 415 ppm, leading to a BT of 24 minutes. The sorbents used here and in Samari's et al. work are different ($Ca(OH)_2$ and CaO, respectively), although the active agent is the same (Ca). A meaningful comparison between both experiments can be made by evaluating the ratio of the mass of CO_2 captured for the duration of the BT and the mass of Ca contained in the sorbent. The results of this evaluation are presented in the last column of table 2 and show that the capture of CO_2 achieved by means of passive hydration was 1.5 times higher than that obtained by forced hydration for 3 hours. However, it must be stressed that the experimental conditions in both tests are different. In particular, nanosilica has been added in the present experiments to facilitate fluidization of the sorbent, which has also an impact on the BT as it allows uniform fluidization.

The content of H_2O vol% in the effluent gas during the CO_2 capture tests was also accurately monitored by means of FTIR. The corresponding results are presented in figure 10, in which CO_2 breakthrough times are marked by a vertical arrow. As expected, the temporal evolution of H_2O is also affected by the storage RH, so that the higher the storage RH the more vapor water is present in the effluent gas.

The presence of H_2O in the effluent gas may have two distinct origins. Firstly, $Ca(OH)_2$ is desiccated by the continuous flow of dry CO_2/N_2 gas passing through the sample during the capture tests. Therefore, a fraction of the H_2O that

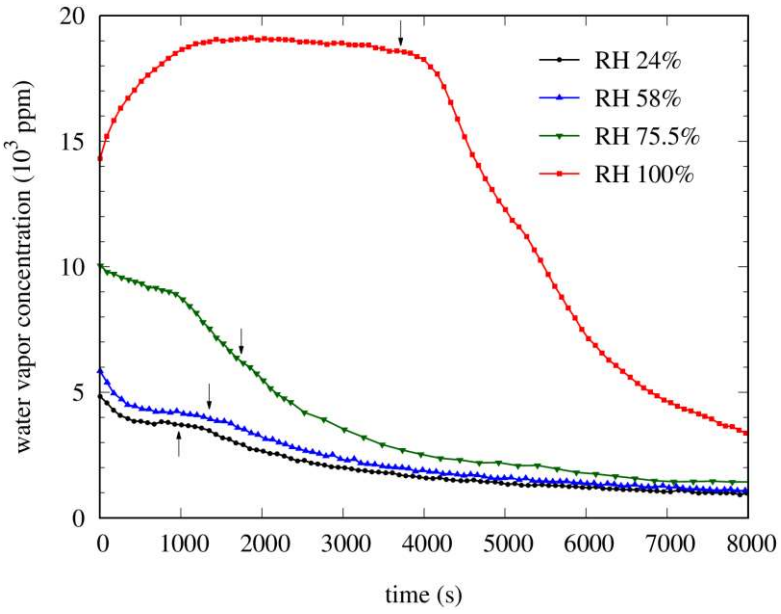

Figure 10: Time evolution of H_2O in the effluent gas during CO_2 capture by $Ca(OH)_2$ samples previously stored at different relative humidities, as indicated. The vertical arrows indicate the CO_2 breakthrough times.

was adsorbed during storage is released during the experiments. Secondly, carbonation of $Ca(OH)_2$ generates additional water, as stated by the global reaction (6).

Remarkably, the time evolution of the H_2O vol% is qualitatively very different in the sample stored at a RH close to 100%. In that case, water vapor increases with time and remains high until the CO_2 breakthrough time is reached (~ 4000 s). Such evolution is a clear indication that the presence of H_2O in the effluent gas is mostly linked to the carbonation of $Ca(OH)_2$. In the rest of samples, the release of H_2O decreases steadily over time but, as will be shown

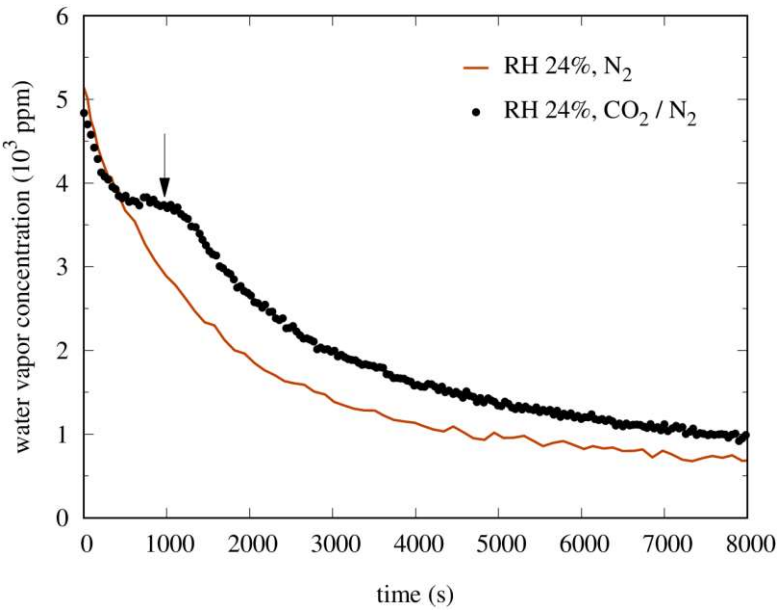

Figure 11: Time evolution of H_2O in the effluent gas using dry N_2 (solid line) and a dry CO_2/N_2 mixture (dots) in $Ca(OH)_2$ samples previously stored at a relative humidity of 24%. The vertical arrows indicate the CO_2 breakthrough time in the capture test.

below, a certain degree of carbonation also occurs, even in samples stored at very low RH.

Figure 11 shows the time evolution of the H_2O vol% in the effluent gas for the $Ca(OH)_2$ sample stored at RH of 24%, using as inflow gas either the dry CO_2/N_2 gas mixture or pure N_2. When N_2 is used in the test (solid line), carbonation is prevented and the presence of H_2O in the effluent gas can only be attributed to the desiccation of $Ca(OH)_2$. In this case, the H_2O vol% decays exponentially in time, as would be expected. However, the result of the actual CO_2 capture test (dots), using the dry CO_2/N_2 gas mixture, shows that the water vapor

concentration follows a different decay pattern. A short initial transient, in which drying is the main source of H_2O, is followed by a much slower decay that extends up to the BT (vertical arrow), approximately. The increase of H_2O vol% with respect to the drying test evidences that carbonation is occurring in this sample, and the same conclusion can also be applied to tests carried out in samples stored at RH of 58% and 75.5%. Nevertheless, in all these samples, carbonation is much less significant than that observed in $Ca(OH)_2$ stored at a RH of 100%, as suggested from the huge presence of water vapor measured in the effluent gas (red squares in figure 10).

In order to quantify precisely the amount of CO_2 that was captured by the carbonation reaction, $Ca(OH)_2$ samples were analyzed using X-ray powder diffractometry after the conclusion of the CO_2 capture tests. During the time between the end of the capture test and the X-ray analysis, the samples were stored in airtight bags, in order to prevent any further carbonation. A $Ca(OH)_2$ sample, as received, was also analyzed for a reference. The diffractograms obtained from the XRD analysis are shown in figure 12. Intensity peaks corresponding to portlandite, $Ca(OH)_2$, and calcite, $CaCO_3$, have been identified with markers inside the figure. Calcite has a very intense main diffraction peak at $2\theta \approx 29.5^{o}$. The inset in figure 12 shows a magnified view of this peak to appreciate the role played by the storage RH conditions. Rietveld refinement was used to calculate quantitatively the portlandite and calcite contents in the

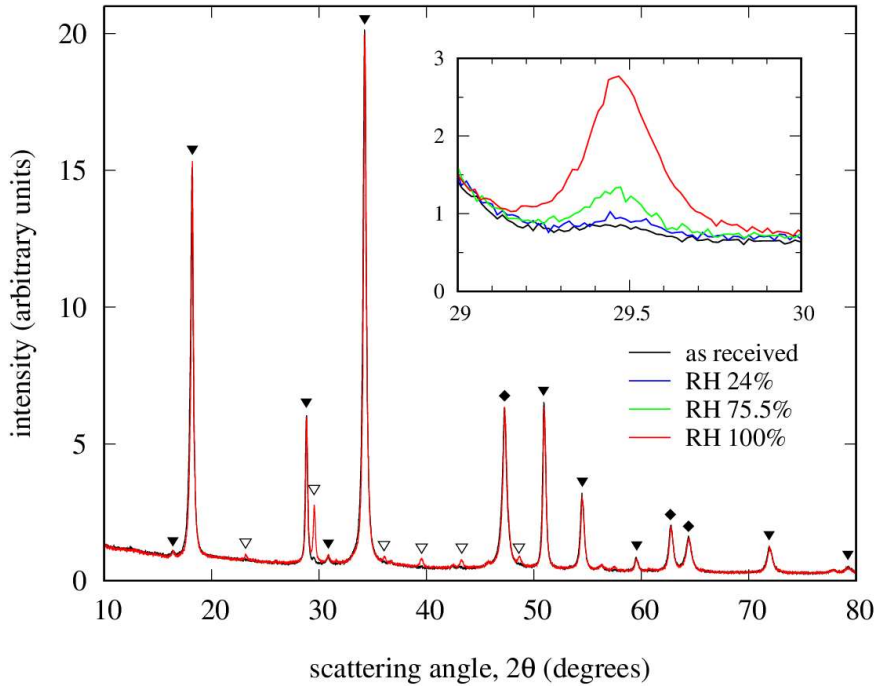

Figure 12: X-Ray diffraction patterns of $Ca(OH)_2$ samples as received, and after being stored at different relative humidities (as indicated) and exposed to a flow of dry CO_2/N_2 (1 vol.% CO_2). For the sake of clarity, only the cases "as received" and RH 100% are shown in the main figure. The inset shows a subset of the scattering angle, corresponding to the most intense peak of calcite ($CaCO_3$). Markers identify the main intensity peaks of portlandite $Ca(OH)_2$ (▼), calcite (▽), and overlapping peaks of portlandite and calcite (◆).

analyzed samples. The variation in $CaCO_3$ mass content with respect to the as received sample can be seen in figure 13 as green bars. Also, the estimated increase in $CaCO_3$ mass content in the samples, assuming that the capture of CO_2 occurred entirely according to the carbonation reaction (6), is presented in figure 13. These data have been calculated from the FTIR measurement of CO_2

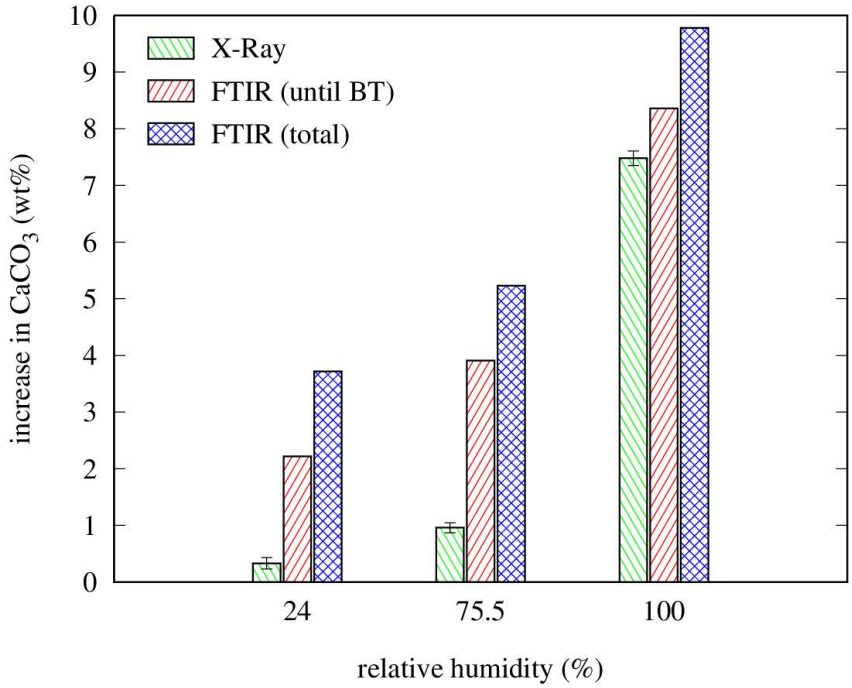

Figure 13: Expected increase in $CaCO_3$ mass according to FTIR analysis (red and blue bars) and actual increase according to X-Ray diffraction analysis (green bars) after CO_2 capture in $Ca(OH)_2$ samples previously stored at different RH conditions (as indicated).

concentration in the effluent gas for the entire duration of the capture test (blue bars) and for the duration of the BT (red bars).

X-ray analysis confirms that carbonation of $Ca(OH)_2$ increases with the RH at which $Ca(OH)_2$ was maintained during the pre-hydration phase. However, while the observed carbonation is weak (below 1%) in samples stored at RH of 24% and 75.5%, it rises up sharply up to 7.5% for 100% storage RH. This last value is similar to the one derived from the FTIR measurement in the BT (8.4%). In contrast, in the other samples (RH of 24% and 75.5%), the expected increase of

$CaCO_3$ according to the FTIR analysis should be much higher than that found from the XRD Rietveld analysis. This apparent disagreement seems to indicate that the capture of CO_2 in these samples occurs mainly through physical adsorption, or that chemisorption of CO_2, if occurs, does not end up as precipitated $CaCO_3$. The contrary is true when the $Ca(OH)_2$ sample was pre-hydrated using a RH of about 100%. In that case, nearly 80% of the CO_2 captured was in the form of $CaCO_3$, which is consistent with the high concentration of H_2O observed in the effluent, as can be expected from the carbonation global reaction expressed by reaction (6).

As previously discussed, water physisorbed during pre-hydration of the samples is the main factor that determines carbonation in experiments. As the carbonation reaction proceeds, a layer of precipitated $CaCO_3$ is formed on the surface of the $Ca(OH)_2$ particles, which hinders the dissolution of further $Ca(OH)_2$ and precludes the diffusion of CO_2 across this barrier. However, in CO_2 capture applications, this limitation can be partially overcome by incorporating water vapor into the CO_2 gas stream. In such a case, physisorption of this extra humidity in non-passivated sites of $Ca(OH)_2$ particles would provide new reactions sites for further carbonation to proceed.

6. Conclusions

This work has investigated how CO_2 capture by a fluidized bed of $Ca(OH)_2$ is affected by previous storage of the sorbent in a controlled humidity environment. The CO_2 capture tests were carried out at ambient temperature and atmospheric pressure using a low CO_2 vol% in the inlet gas flow, in order to assess the performance of these samples for DAC. Pre-hydration of the sorbent during storage was achieved by passive exposure to a variety of accurately controlled relative humidities, belonging to a wide range of environments from very dry to close to dew point. Results from CO_2 capture tests have shown that the storage RH has a critical effect on the CO_2 breakthrough time and hence on the overall CO_2 capture capacity of the sample: the higher the storage RH, the longer the breakthrough time and the greater the mass of CO_2 captured. However, the correlation between the CO_2 capture capacity and the storage RH is not linear, which is related to the mechanism that governs physisorption of water in $Ca(OH)_2$ at room temperature. Samples stored at RH close to 100% exhibited much higher capture capacities and extraordinarily prolonged CO_2 breakthrough times. X-ray powder diffractometry has revealed that, in these samples, most of CO_2 capture occurs by carbonation. In contrast, for lower storage RH ($\leq$ 75 %), carbonation contributes only by a small fraction to CO_2 capture. In this case most of the CO_2 captured is probably dissolved or in the form of bicarbonate ions in the physisorbed water present in $Ca(OH)_2$.

Moreover, samples stored at 100% RH exhibit an improved fluidization behavior as revealed by bed expansion measurements, which would favor the gas solid interaction and therefore enhance CO_2 capture. From these measurements, it can be concluded that pre-hydration of $Ca(OH)_2$ during its storage at high RH greatly enhances its capture performance at ambient conditions, which is relevant for the use of this sorbent in DAC applications.

7. Acknowledgements

This research was supported by the Spanish Government Agency "Ministerio de Economía y Competitividad" (grant number CTQ2017-83602-C2-2-R). The authors gratefully acknowledge the technical assistance of the services of the Innovation, Technology and Research Center of the University of Seville (CITIUS).

8. References

[1] J. Rogelj, Gu. Luderer, R. C. Pietzcker, E. Kriegler, M. Schaeffer, V. Krey K. Riahi, Energy system transformations for limiting end-of-century warming to below 1.5 °C, *Nature Climate Change* **5** (2015) 519-528.

[2] J. Blamey, E. J. Anthony, J. Wang, P. S. Fennell, The calcium looping cycle for large-scale CO_2 capture, *Progress in Energy and Combustion Science* **36** (2010) 260-279.

[3] D. Y. C. Leung, G. Caramanna, M. M Maroto-Valer, An overview of current status of carbon dioxide capture and storage technologies, *Renewable and Sustainable Energy Reviews* **39** (2014) 426-443.

[4] IEA (2017), CO_2 Emissions from Fuel Combustion 2017, OECD Publishing, Paris, https://doi.org/10.1787/co2_fuel-2017-en.

[5] J. Tollefson, The 2 ºC dream, *Nature* **527** (2015) 436-438.

[6] J. C. Minx, W. F. Lamb, M. W. Callaghan, S. Fuss, J. Hilaire, F. Creutzig, T. Amann, T. Beringer, W. de Oliveira Garcia, J. Hartmann, T. Khanna, D. Lenzi, G. Luderer, G. F. Nemet, J. Rogelj, P. Smith, J. L. Vicente Vicente, J. Wilcox, M. del Mar Zamora Dominguez, Negative emissions-Part 1: Research landscape and synthesis, *Environmental Research Letters*, **13** (2018) 063001.

[7] H. de Coninck *et al.*, Strengthening and Implementing the Global Response. In: *Global Warming of 1.5°C. An IPCC Special Report on the impacts of global warming of 1.5°C above pre-industrial levels and related global greenhouse gas emission pathways, in the context of strengthening the global response to the threat of climate change, sustainable development, and efforts to eradicate poverty*. Masson-Delmotte *et al.* (eds.), 2018. (https://www.ipcc.ch/sr15/)

[8] S. Fuss *et al*. Betting on negative emissions, *Nature Climate Change* **4** (2014) 850-853.

[9] H. Mandova, P. Patrizio, S. Leduc, J. Kjärstad, C. Wang, E. Wetterlund, F. Kraxner, W. Gale, Achieving carbon-neutral iron and steelmaking in Europe through the deployment of bioenergy with carbon capture and storage, *Journal of Cleaner Production* **218** (2019) 118-129.

[10] C. W. Jones, CO_2 capture from dilute gases as a component of modern global carbon management, *Annual Review of Chemical and Biomolecular Engineering* **2** (2011) 31-52.

[11] A. Marcucci, S. Kypreos, E. Panos, The road to achieving the long-term Paris targets: energy transition and the role of direct air capture, *Climatic Change* **144** (2017) 181-193.

[12] M. Fasihi, O. Efimova, C. Breyer, Techno-economic assessment of CO_2 direct air capture plants, *Journal of Cleaner Production* **224** (2019) 957-980

[13] S. Talukdar, N. Banthia, Carbonation in concrete infrastructure in the context of global climate change: Development of a service lifespan model, *Construction and Building Material* **40** (2013) 775-782.

[14] A. Goeppert, M. Czaun, G. K. S. Prakash and G. A. Olah, Air as the renewable carbon source of the future: an overview of CO_2 capture from the atmosphere, *Energy & Environmental Science* 5 (2012) 7833-7853.

[15] L. K. G. Bhatta, S. Subramanyam, M. D. Chengala, S. Olivera, K. Venkatesh, Progress in hydrotalcite like compounds and metal-based oxides for CO_2 capture: a review, *Journal of Cleaner Production*, **103** (2015) 171-196

[16] D. P. Hanak, E. J. Anthony, V. Manovica, A review of developments in pilot-plant testing and modelling of calcium looping process for CO_2 capture from power generation systems, *Energy & Environmental Science* **8** (2015) 2199-2249.

[17] A. Perejón, L. M. Romeo, Y. Lara, P. Lisbona, A. Martínez, J. M. Valverde, The Calcium-Looping technology for CO_2 capture: On the important roles of energy integration and sorbent behavior, *Applied Energy* **162** (2016) 787-807

[18] C. Ortiz, J. M. Valverde, R. Chacartegui, L. A. Perez-Maqueda, Carbonation of limestone derived CaO for thermochemical energy storage: From kinetics to process integration in concentrating solar plants, *Sustainable Chemistry & Engineering* **6** (2018) 6404- 6417.

[19] F. N. Ridha, V. Manovic, A. Macchi, E. J. Anthony, CO_2 capture at ambient temperature in a fixed bed with CaO-based sorbents, *Applied Energy* **140** (2015) 297-303.

[20] M. Erans, S. A. Nabavi, V. Manovi, Carbonation of lime-based materials under ambient conditions for direct air capture, *Journal of Cleaner Production* **242** (2020) 118330.

[21] S. M. Shih, C. H. Ho, Y. S. Song, J. P. Lin, Kinetics of the reaction of $Ca(OH)_2$ with CO_2 at low temperature, *Industrial & Engineering Chemistry Research* **38** (1999) 1316–1322.

[22] M. Samari, F. Ridha, V. Manovic, A. Macchi, E. J. Anthony, Direct capture of carbon dioxide from air via lime-based sorbents, *Mitigation and Adaptation Strategies for Global Change* (2019). https://doi.org/10.1007/s11027-019-9845-0.

[23] R. M. Dheilly, J. Tudo, Y. Sebaı bi, M. Queneudec, Influence of storage conditions on the carbonation of powdered $Ca(OH)_2$, *Construction and Building Materials* **16** (2002) 155–161.

[24] F. Pontiga, J. M. Valverde, H. Moreno, F. J. Duran-Olivencia, Dry gas–solid carbonation in fluidized beds of Ca(OH)2 and nanosilica/$Ca(OH)_2$ at ambient temperature and low CO_2 pressure, *Chemical Engineering Journal*, **222** (2013) 546-552.

[25] L. Greenspan, Humidity fixed points of binary saturated aqueous solutions, *Journal of Research of the National Bureau of Standards - A. Physics and Chemistry*, **81A** (1977) 89–96.

[26] D. T. Beruto, R. Botter, Liquid-like H_2O adsorption layers to catalyze the $Ca(OH)_2/CO_2$ solid–gas reaction and to form a non-protective solid product layer at 20 ºC, *Journal of the European Ceramic Society* **20** (2000) 497–503.

[27] A. M. Kalinkin, E. V. Kalinkina, O. A. Zalkind, T. I. Makarova, Chemical interaction of calcium oxide and calcium hydroxide with CO_2 during mechanical activation, *Inorganic Materials,* **41** (2005) 1218–1224.

[28] G. Montes-Hernandez, A. Pommerol, F. Renard, P. Beck, E. Quirico, O. Brissaud, In situ kinetic measurements of gas–solid carbonation of $Ca(OH)_2$ by using an infrared microscope coupled to a reaction cell, *Chemical Engineering Journal*, **161** (2010) 250–256.

[29] D. Geldart, Types of gas fluidization, *Powder Technology* **7** (1973) 285–293.

[30] M. Seipenbusch, S. Rothenbacher, M. Kirchhoff, H.-J. Schmid, G. Kasper, A. P. Weber, Interparticle forces in silica nanoparticle agglomerates, *Journal of Nanoparticle Research* **12** (2010) 2037–2044.

[31] J. M. Valverde, F. Pontiga, C. Soria-Hoyo, M. A. S. Quintanilla, H. Moreno, F. J. Duran, M. J. Espin, Improving the gas–solids contact efficiency in a fluidized bed of CO_2 adsorbent fine particles, *Physical Chemistry Chemical Physics* **13** (2011) 14906-14909.

[32] J. M. Valverde, F. J. Duran, F. Pontiga and H. Moreno, CO_2 capture enhancement in a fluidized bed of a modified Geldart C powder, *Powder Technology* **224** (2012) 247–252.

[33] M. Thommes, K. Kaneko, A. V. Neimark, J. P. Olivier, F. Rodriguez-Reinoso, J. Rouquerol and K.W. Sing, Physisorption of gases, with special reference to the evaluation of surface area and pore size distribution (IUPAC Technical Report), *Pure and Applied Chemistry* **87** (2015) 1051-1069.

[34] D. C. Hughes and J.M. Illingworth, Low energy pre-blended mortars: Part 1 – Control of the sand drying process using a lime drying technique, *Construction and Building Materials* **101** (2015) 466-473.

[35] C. Soria-Hoyo, J. M. Valverde and A. Castellanos, Avalanches in moistened beds of glass beads, *Powder Technology* **196** (2009) 257–262.

[36] J. Perez-Vaquero, J. M. Valverde and M. A. S. Quintanilla, Flow properties of CO_2 sorbent powders modified with nanosilica, *Powder Technology* **249** (2013) 443–455.

[37] G. M. Bond, J. Stringer, D. K. Brandvold, F. A. Simsek, M.-G. Medina and G. Egeland, Development of integrated system for biomimetic CO_2 sequestration using the enzyme carbonic anhydrase, *Energy & Fuels* **15** (2001) 309-316.

[38] C. A. J. Appelo and D. Postma, *Geochemistry, Groundwater and Pollution*, Ed. A. A. Balkema Publishers, The Netherlands, 2005.